Point Clouds: Lidar versus 3D Vision

F. Leberl, A. Irschara, T. Pock, P. Meixner, M. Gruber, S. Scholz, and A. Wiechert

Abstract

Novel automated photogrammetry is based on four innovations. First is the cost-free increase of overlap between images when sensing digitally. Second is an improved radiometry. Third is multi-view matching. Fourth is the Graphics Processing Unit (GPU), making complex algorithms for image matching very practical. These innovations lead to improved automation of the photogrammetric workflow so that point clouds are created at sub-pixel accuracy, at very dense intervals, and in near real-time, thereby eroding the unique selling proposition of lidar scanners.

Two test projects compare point clouds from aerial and street-side lidar systems with those created from images. We show that the photogrammetric accuracy compares well with the lidar-method, yet the density of surface points is much higher from images, and the throughput is commensurate with a fully automated all-digital approach. Beyond this density, we identify 15 additional advantages of the photogrammetric approach.

Introduction

Lidar Emergence

Lidar point clouds have conquered a major position ever since point clouds have become a mapping data product in its own right (Shan and Toth, 2009). Image-based stereo-photogrammetric point clouds could not compete on price and throughput. The advantages of one method over the other have been the topic of studies and discussions during the last decade. Baltsavias (1999) was an early advocate of lidar as the superior approach to the creation of terrain elevation data from an aerial platform. Bitelli *et al.* (2004) clearly preferred the terrestrial lidar-method over aerial photogrammetry in detailed terrain studies for landslides. Wang *et al.* (2009) state that lidar is "*rapidly replacing the photogrammetric approach.*" However, practical experiments by Veneziano *et al.* (2002) and Choma *et al.* (2005) were less enthusiastic about lidar and found that there was a continued role for stereo-photogrammetry. Service providers also suggest a role for each approach (Beasy, 2007). A clarity of conclusions is missing in many of the more recent studies, for example by Champion *et al.* (2009). A large European project by Kaartinen *et al.* (2005) also remains inconclusive.

A preferred recommendation by academic researchers is to combine lidar with image analysis (Habib *et al.*, 2005). Optech (2009) is offering a product of "active vision" to support this approach. However, in these suggestions the 3D measurement remains a domain of the lidar approach; the images serve as a 2D augmentation.

Lidar Momentum

Recently, lidar has gained enormous momentum: 440 aerial lidar-systems appear to currently be in practical use, exceeding by a large margin the about 270 large format digital aerial cameras. Petrie (2009) estimates that about 280 systems have been sold by Leica Geosystems and Optech, Inc.; a Riegl, Inc. source lists their install-base at 140 units; and another 20 systems have been built by other enterprises. Considering the economy of these investments, the mapping business based on lidar sensors should globally exceed that built on large format digital cameras. Since lidar only maps in 3D and photogrammetry produces both 2D and 3D data, it appears that lidar dominates the 3D business.

The momentum towards lidar solutions is also documented by the density of technical and scientific publications, conferences, and training courses on laser scanning versus photogrammetric research papers (ILMF, 2009; ASPRS, 2009; DGPF, 2009). Imagery serves in many cases merely to provide photographic color texture for orthophotos and for three-dimensional (3D) object models created by lidar. The importance and volume of photogrammetric work seems to erode as the acceptance of, and interest in, lidar-type data increases.

Intersecting Projection Rays versus Direct Distance and Angle Measurements

The defining capability of the [stereo-] photogrammetric method was to measure an object's geometry, in particular its 3D-shape, from multiple image-based projection rays (McGlone *et al.*, 2004). The interest in 3D point clouds would thus appear at first sight to fit with an application of the photogrammetric method. However, if the measurement of 3D shape becomes the domain of direct distance and direction measurements by lidar systems, then the intersecting projection rays effectively lose their usefulness, certainly for this application. What then will be the value of photogrammetric methods?

If previous photogrammetric centers of excellence direct their innovation resources towards lidar, then the result is a decline of image-based photogrammetry innovation. Fortunately, this gap is being filled by computer vision as the driving force for new image analysis ideas and innovation in 3D object shape measurements.

F. Leberl, A. Irschara, T. Pock, and P. Meixner are with the Graz University of Technology, Institute for Computer Graphics and Vision, Inffeldgasse 16, A-8010 Graz, Austria (leberl@icg.tugraz.at).

M. Gruber, S. Scholz, and A. Wiechert are with Microsoft Photogrammetry, Anzengruberstrasse 8, A-8010 Graz, Austria.

Photogrammetric Engineering & Remote Sensing
Vol. 76, No. 10, October 2010, pp. 1123–1134.

0099-1112/10/7610–1123/$3.00/0

Recent Changes in Image-based Measurement Methods

A series of changes has occurred in photogrammetry-proper since lidar has first become an accepted, even preferred, 3D sensor. Novel digital large format aerial cameras produce significantly improved image quality and no-cost increases of overlapping imagery. This in turn creates the ability to automate previously manual processes, and it sets new standards of economy. Simultaneously, computer vision has produced various algorithmic innovations in multi-image matching and multi-image-based point cloud measurements. Also, computer vision has begun to take advantage of the invention of the Graphics Processing Unit (GPU, see **www.nvidia.com**), opening the door to significant economic benefits. We are examining in this paper how these facts affect the balance between the results from lidar surveys versus those from a photogrammetric imaging campaign in the application to point cloud measurements. We conclude that novel photogrammetric approaches deliver point clouds at comparable accuracy but higher density and superior throughput than lidar. Given the advantages of a single workflow and the existence of images for a variety of applications, we find that image-based methods are superior to lidar-surveys in the creation of 3D point clouds.

Terminology: Lidar, 3D Vision, and Softcopy Photogrammetry

The photogrammetric text book by Kraus (2004) defines lidar as a part of photogrammetry. It thereby avoids contrasting lidar with photogrammetry. But is lidar a photogrammetric technology?

We avoid confusion if we specify the image-based approach more explicitly. We achieve this with the term "softcopy photogrammetry," which clearly refers to a softcopy image and excludes lidar. However, softcopy photogrammetry is an all-encompassing term to address both 3D as well as 2D applications. Furthermore, softcopy photogrammetry does not reflect the advent of computer vision as a force of innovation, and with its own terminology.

We find the term "3D Vision" helpful for two reasons. First, it clearly only is image based, as implied by the word *vision.* Second, it reflects its genesis in computer science and computer vision. The term 3D Vision denotes the part of computer vision dealing with 3D object shapes, 3D point clouds, and, as a specialization, with DSMs and DTMs. We will argue that 3D vision and 3D image-based photogrammetry are synonyms. In the remainder of this paper, we prefer the shorter expression.

About Aerial Lidar

The Appeal of Instant Gratification

In the world of film imaging, a 3D point cloud came at the end of a long workflow that started in the air with heavy and costly rolls of environmentally fragile film, proceeded to the photo lab for film development, went through scanning of the film images, then through a manually-supported aerial triangulation (AT), and achieved the point cloud in smaller patches by two-image stereo matches from pairs of images with 60 percent stereo overlap (McGlone *et al.*, 2004). These patches were being merged using the results of the triangulation so that a large area was being covered in a seamless assembly of patches representing a single point cloud. The time from taking the images to actually seeing the digital terrain model spanned weeks.

In this world, the direct assembly of point clouds from lidar systems appeals, because the time from sensing to actually inspecting a surface model is reduced to almost zero, offering instant gratification: no film, no film-to-pixel-conversion, and no matching. The point cloud is viewable as it gets downloaded from the sensor.

Lidar is predicated on the use of the global positioning system (GPS) and an inertial measuring unit (IMU) to position and orient the sensor in a 3D World Geodetic System 1984 (WGS84). This reliance on direct geo-referencing is seen as a second major advantage because there is no need for any type of triangulation and thus saving elapsed time and manual labor. However, photogrammetric workflows often use GPS/IMU for the avoidance of AT and ground control measurements. Yet, total reliance on GPS/IMU does compromise the accuracy of the resulting stereo matches and point cloud patches. Similarly, accuracy limitations of the GPS/IMU positioning/orientation will cause geometric mismatches in the lidar data along the overlapping seams of separately collected data strips, which will need to be removed by some adjustment with manual intervention. While a new point cloud will indeed be created quickly by lidar, the subsequent manually-supported postprocessing will compromise the instant gratification (Schickler and Thorpe, 2001), and so will the need to extract mapping objects from the points (Grün, 2007).

The Appeal of Vegetation Penetration

A frequently made argument in favor of aerial lidar scanning builds on the ability of a lidar sensor to produce multiple reflections by one single pulse, creating a surface of the bald earth and separately mapping the top of all objects on the bald earth. This is the classical forestry application of lidar scanning (ILMF, 2009). However, most photogrammetric software systems for the creation of DSMs offer a module for filtering of the bald earth (DSM → DTM). We are not aware of any thorough studies that would show how well 3D vision succeeds in separately mapping the bald earth and its vertical objects. An opinion that 3D vision is unable to deliver bald earth data at a lidar-level of accuracy needs to be examined and contrasted with the ability of mapping vegetation with its properties. Hirschmugl (2008) has successfully applied multi-view aerial photography to individual tree and forest mapping.

The Cost and Quality of Aerial Lidar Operations

Aerial lidar point density may be in the range of 1 to 5 points/m^2. Aerial photogrammetry point density may at first be seen as defined by the two-dimensional (2D) ground sampling distance (GSD), thus pixel size. At a 10 cm pixel, one would produce 100 points/m^2, but these are not 3D elevation values. The 3D sampling interval depends on the image overlap to achieve independent 3D matches. If 50 percent of the pixels were to get matched for independent 3D elevation values, one would achieve 50 points/m^2 from 10 cm pixels.

The difference between lidar and 3D image-based photogrammetry is more distinct when one considers swath width and flight lines. Table 1 presents some typical 2009 project values for a lidar system flying at 750 meters above ground at 60 m/sec. It needs to fly slowly to not obtain too

Table 1. Project Parameters for a Lidar and a Digital Photogrammetric Camera; Status 2009

LIDAR	DIGITAL PHOTOGRAMMETRY
170 scans per second (190 kHz), 30° FOV;	GSD 25 cm
8 points/m^2	16 points/m^2
Flying height 750 meters	Flying height 4,188 m
Aircraft speed 60 m/sec	*Aircraft speed 141 m/sec*
Strip width 403 m	Strip width 4328 m
20% side-lap between flight lines	60% side-lap between flight lines
Effective strip width at 322 m	*Effective strip width 1,731 m*

wide a spacing of points in flight direction. The flight lines are 322 meters apart. An equivalent photogrammetric system is a digital camera flying at ~4,000 meters for a pixel size of 25 cm and at an aircraft speed of 140 m/sec. Aircraft speed is not really a factor for fast digital frame cameras The flight lines are 1,730 m apart.

Under these assumptions we would have to be in the air 13 times longer with a lidar than with a camera to obtain comparable elevation results. First, the aircraft speed would be 2.5 times lower for the lidar than for the camera; second, the lidar swath width would be about $1/6^{th}$ of the camera's. These differences in economy are further aggravated by the lidar suffering more occlusions with 20 percent overlap than the camera flown at a 60 percent side-lap. At comparable occlusions, the image advantage would grow to a factor 26.

The camera GSD at 25 cm in Table 1 produces a lidar-type point density. However, this GSD is insufficient in a quest to interpret all urban objects. More likely is a GSD at 15 cm and down to 8 cm. At those values the objects get defined by 100 points/m^2. However, as the photogrammetric point density increases, so does the flying cost due to additional flight lines at lower altitude. Improving the pixel size to 12 cm reduces the economic advantage of the camera's flying operation to a mere value of 6; still an impressive difference. When one compares the conclusions from Table 1 with the analysis by Baltsavias (1999), one will note that the system specifications for both lidar and camera systems have significantly changed. Of the seven major advantages of lidar over photogrammetry presented by Baltsavias in 1999, five have been eroded by innovations.

Digital Aerial 3D Photogrammetry

Dramatic potential for advances in photogrammetric technology are emerging in the transition to the now all-digital workflow, characterized by digital aerial cameras and fully automated procedures. Making these advantages work in everyday practice is a challenge currently faced by the commercial vendors of photogrammetric systems.

We have identified six separate areas of progress and innovation. Some of these need yet to leave the academic research domain towards everyday practice. For example multi-image matching for terrain modeling is not yet widely available, and early implementations typically do not really deserve that designation since they oftentimes simply repeat a two-image stereo match and then fuse the multiple two-image results by some sort of averaging.

From Film to Digital Aerial Cameras

Probably the most striking change resulting from a film-to-digital transition is in the *radiometric capabilities.* Film has traditionally been scanned at a resolution of 8-bits, with hardly ever fully performing at 256 grey levels (Perko, 2004). By contrast, digital sensors have been shown to produce almost 13 bits and thus in excess of 7,000 grey values, as shown in Figure 1 (Scholz and Gruber, 2008).

The notorious *grain noise* does affect the geometric resolution of film imagery. With effective geometric pixel sizes in the range of 20 μm at 8-bits per color band and with a 25 cm image width, an aerial film image is being fully represented by 11,500 pixels (Perko, 2004; Perko *et al.*, 2004). There exists a complex dependency between the radiometric range (at 256 grey values) and the geometric pixel size (at 20 μm). Smaller pixel sizes, say at 15 μm, will result in a reduced radiometric range of far less than 8-bit. A radiometry range encompassing the full 8-bit may only be achieved with ~30 μm pixels (Perko, 2004). This gives a vast advantage to the digital sensor with small CCD elements at 6.2 μm, combined with a signal-to-noise ratio at 72 db or 12- to 13-bits (Scholz and Gruber, 2009).

Smart Image Acquisition Strategies

Since its inception, photogrammetry was driven by minimizing the number of (film) images for any given project. Every additional image caused additional cost for materials, additional labor for dealing with the image, and resulted in yet another stereo model to be manually processed. A surface point was defined by two optical rays, representing four equations to solve for the three unknown coordinates *x*, *y*, and *z.* These four equations for three unknowns have led to a photogrammetric workflow that hardly satisfied the surveyor's rule for reasonable redundancy. The transition to digital sensing did away with the extra cost for extra imagery. Automation does away with extra labor per image. Multi-view geometry does away with the idea that an additional image necessitates additional work with an additional stereo model (Hartley and Zisserman, 2004).

Images can now be produced at 80 percent forward overlap, increasing the number of images per object point from two to five, at absolutely no additional cost of acquisition. At 90 percent forward overlap, the number of images

Figure 1. 7,860 grey values between darkest and brightest regions in each 6.2 μm pixel (UltraCamX).

per object point within a flight line grows to ten. And by an increase of the side-lap from the traditional 20 percent to now 60 percent, the add-on cost will increase only for the additional air time, but not for the increase in the number of images. The strategy increases the number of images per object point to 10 (at an 80 percent overlap) or even 20 (at a 90 percent overlap). The benefits are numerous: reduced occlusions, higher level of automation (see below), reduced occurrence of blunders/gross errors and therefore less manual editing, and finally an increase of geometric accuracy (see also below).

Automated Triangulation
Photogrammetric operations have long benefitted from direct geo-referencing of aerial imagery based on GPS-positions and IMU-attitudes (Ackermann, 1993). Those benefits are in the reduction of the number of ground control points, and at times even the avoidance of any aerial triangulation and replacement by dead-reckoning, also denoted as direct geo-referencing.

Highly Overlapping Large Image Blocks are Rigid Structures
However, if one plans the extraction of a dense digital terrain model from a block of imagery, then an AT is necessary to obtain the best possible sub-pixel accuracy in the orientation of each image, to avoid any false parallaxes, and to ensure a seamless match of separately collected surface patches. The high-overlap/high redundancy-paradigm presents the challenge for an automated process to avoid a variable labor cost per image. A small city of 150 km^2 will be covered by 3,000 images with 80/60 overlap with 8 cm pixels, resulting in 1.5 TBytes of data (Figure 2). Such data sets do call out for intelligent tools of interaction and automation. Fortunately, the high overlaps increase the chances to successfully match tie-points and to avoid undetected gross errors. In addition, the high overlaps also reduce the need for dense ground control because the image block represents a more rigid structure than a 60 percent forward and 20 percent side-lap would produce. A block with smaller overlaps would be more strongly deformed by undetected systematic and so-called pseudo-systematic errors (Kraus, 2004). As the image overlaps increase, these systematic effects can be more accurately modeled so that very small unit errors of measurement are being achieved.

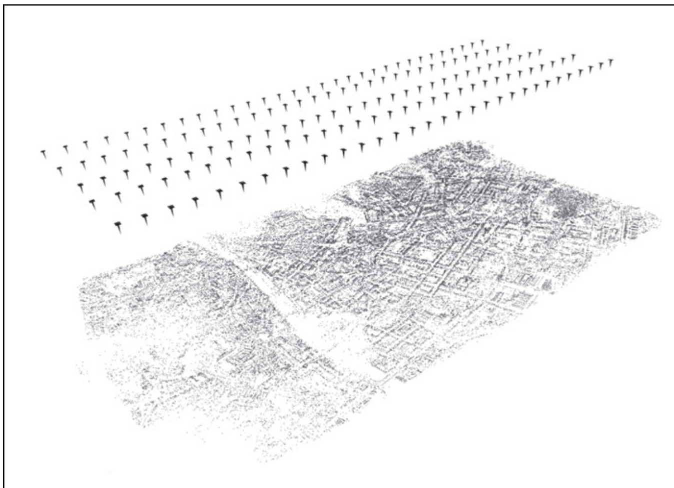

Figure 2. Fully automated AT delivers exterior orientation of thousands of camera stations and 3D *X*, *Y*, *Z* of 1,000's of tie points per image (UltraCam-coverage).

Interacting with a Large Numbers of Images
Any remaining interactive work with images will benefit greatly from tools to work with large numbers of images, even e.g. 1.5 TBytes for 3,000 digital aerial images in one single project. Seadragon was the original technology available from Microsoft™ to deal with very large, multi-terabyte spatial data sets (Agüera y Arcas, 2007; Microsoft Livelabs, 2009). Dragonfly was developed from Seadragon for overlapping aerial photography by generalizing the system to four color bands at 16 bits for each band, and by permitting the images to overlap (Reitinger *et al.*, 2008). This has evolved into a product for automated AT denoted as UltraMap-AT (Gruber, and Reitinger, 2009).

Geometric Accuracies
The high overlap improves the internal accuracies. Such accuracies are commonly described by the σ_0–value of an aerial triangulation, representing the unit error of measurement, thus of the image matches. Figure 3 presents rather remarkable consistent small values for a number of image blocks flown over a long period of time and with 33 different cameras, demonstrating the ability to model all systematic errors because of the use of large image overlap.

Ladstätter and Gruber (2008) have shown that a σ_0–value of $\sim \pm 1$ μm is being achieved. These internal accuracies are better than those traditionally found in film-based photogrammetry. Kraus (2004) in his text book states that σ_0–values should be expected to be in the range of ± 3 μm, i.e., three times worse than with novel digital cameras.

Dense Matching
We denote by dense matching a match of multiple digital images at intervals as small as a pixel. Traditional digital photogrammetry based on two images created matches for terrain models perhaps at an interval like a human stereo operator may use, namely of 10 to 20 pixels, arguing that adjacent pixels will not produce independent surface measurements (Balce, 1986), and that elevation postings should be at a distance that is a multiple of the vertical error of each posting, resulting in a spacing at ten or more pixels. Such relatively sparse grids were manually augmented by surface break lines. But when there are 10 to 20 images per ground point, the traditional rules are no longer meaningful.

Let us consider that we have ten overlapping images. These result in 45 independent point measurements as we could create 45 separate stereo pairs. The argument can be made that 45 observations will result in an improvement by a factor of 7 in the elevation error, compared to having just a single observation. Therefore, the elevation postings

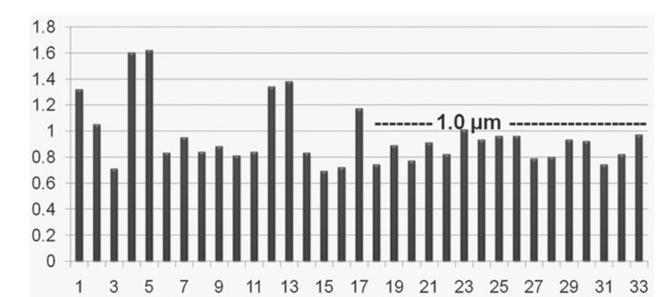

Figure 3. σ_o measures the internal accuracy of the AT. Using 33 cameras, $\sigma_o < \pm 1$ μm.

can be at a much shorter spacing, perhaps at $1/7^{th}$ that used for a single two-image measurement. One might consider this to be analogous to the idea of a so-called super-resolution, a concept in computer vision that describes how merged multiple images at one geometric resolution will result in a combined image at a higher resolution (Irani and Peleg, 1991). Meaningful matches will thus not be achieved only at a ten-pixel interval, but at a spacing of one to two pixels.

A practical approach of multi-view matching is to define image triplets for the creation of surface patches. These patches overlap, so that individual patches need to be fused or merged. Robust fusion methods employ cost functions and variational methods (Zebedin *et al.*, 2009). Figure 4 illustrates a dense match at an interval of two pixels from a ten-image overlap. Of interest is also the ability to strip from the measured point clouds the objects on top of a terrain surface. This is achieved in a filtering process that starts off by defining a coarse point network at minimum heights to describe a bald earth. The technique used in Figure 4 has not been published but generally follows the approach described previously by Zebedin *et al.* (2006). A novel approach uses image-based edge information, separate from the pixel-based matches. This would densify the effective posting interval, if the elevation grids from images get complemented by 3D edges along elevation discontinuities, for example along roof lines of buildings. Bauer (2009) has recently published an original approach to create edge clouds in analogy to point clouds, and has applied analysis methods to find objects in edge clouds.

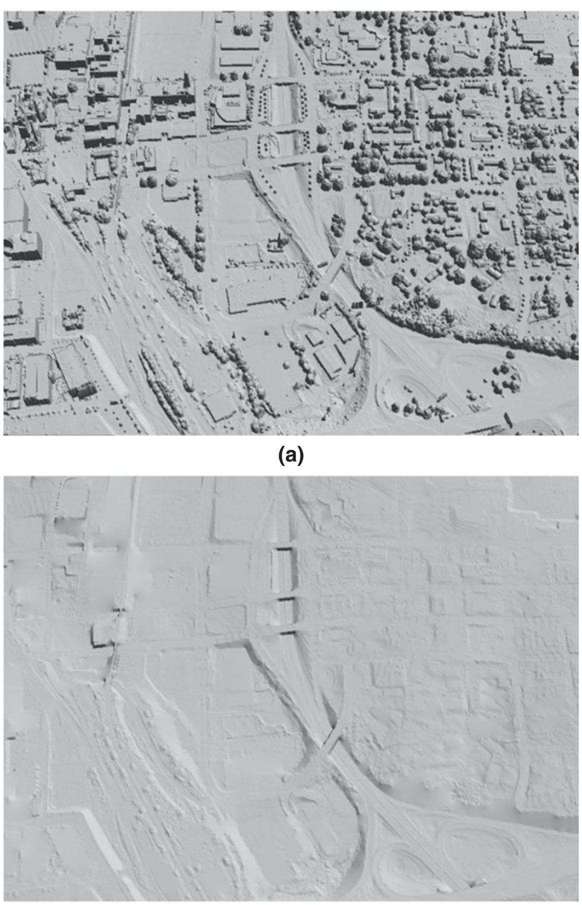

(a)

(b)

Figure 4. (a) A digital surface model DSM, and (b) filtered bald Earth DEM; Winston-Salem (USA), 930 m * 930m; GSD at 15 cm.

Geometric Accuracy

Gruber and Ladstätter (2006) have presented an experiment with eight images defining a surface point. If one reduces the number of images from the initial eight to just two, the vertical uncertainty increases from ±0.6 pixels to about ±3 pixels, thus by a factor of 5 (Gruber and Ladstätter, 2006). This is consistent with the model of improvement from multiple measurements with normally distributed errors. Eight images support 28 independent stereo pairs, resulting in an error reduction by a factor of 5. This is a very relevant difference since, for example, a roof line in a building model will be far better defined from eight rays than from the two rays typically used in the two-image stereo photogrammetric tradition. The higher accuracy is needed especially along various types of discontinuous height features and also substitutes for the traditional collection of terrain break lines.

Limitless Detail by High Geometric Resolution

It certainly is worth noting that the absence of significant variable costs of imaging supports the idea of reducing the pixel size beyond the scale one would select in traditional photogrammetry. In the development of 3D urban building models, one really has no tradition for selecting the proper pixel size; this is uncharted terrain. Based on strictly a geometric accuracy measure, say at ±20 cm, and on the assumption of a system uncertainty in the pixel range, one might be led to a pixel size at 20 cm. And yet, this pixel size will lead to an undesirable lack of crispness of roof lines and other sharp discontinuities, and it will obstruct the interpretation of small man-made objects. The improvement of the image resolution to 10 cm will produce considerably crisper transitions at such discontinuities, and ultimately a superior 3D data product. One can thus observe that a municipal area of 150 km^2 that was imaged by film on 160 images, currently gets imaged by a digital camera onto 3,000 images, both because of an improved GSD as well as increased overlap.

Experimental Comparison of Aerial 3D Vision and Aerial Lidar

A rather large experimental effort has succeeded to collect test data for investigations of new aerial sensors near the University of Stuttgart (Germany) at Vaihingen. Cramer and Haala (2009) and Haala and Wolf (2009) describe the test site and data, as well as some initial analysis results. Aerial lidar and aerial digital camera data have been made available to an international team of study partners. We report here the results obtained by our group. Figure 5 superimposes an image taken with the UltraCamX digital aerial camera with the lidar point cloud taken with the Leica Geosystems ALS50 lidar. The lidar points have been collected at an interval of 45 cm across and 70 cm along the flight path. This produces a formal density of 4 laser points/m^2. The underlying aerial photograph is at 8 cm per pixel or 156 pixels/m^2.

Figure 6 compares a building detail from the laser point cloud to the 3D cloud of photogrammetrically matched points. We have three accuracy observations. First is the photogrammetric aerial triangulation with a σ_o at $\sim \pm 1$ μm or at ±1.1 cm on the ground, using CCD-elements with 6.2 μm. This measurement accuracy needs to be

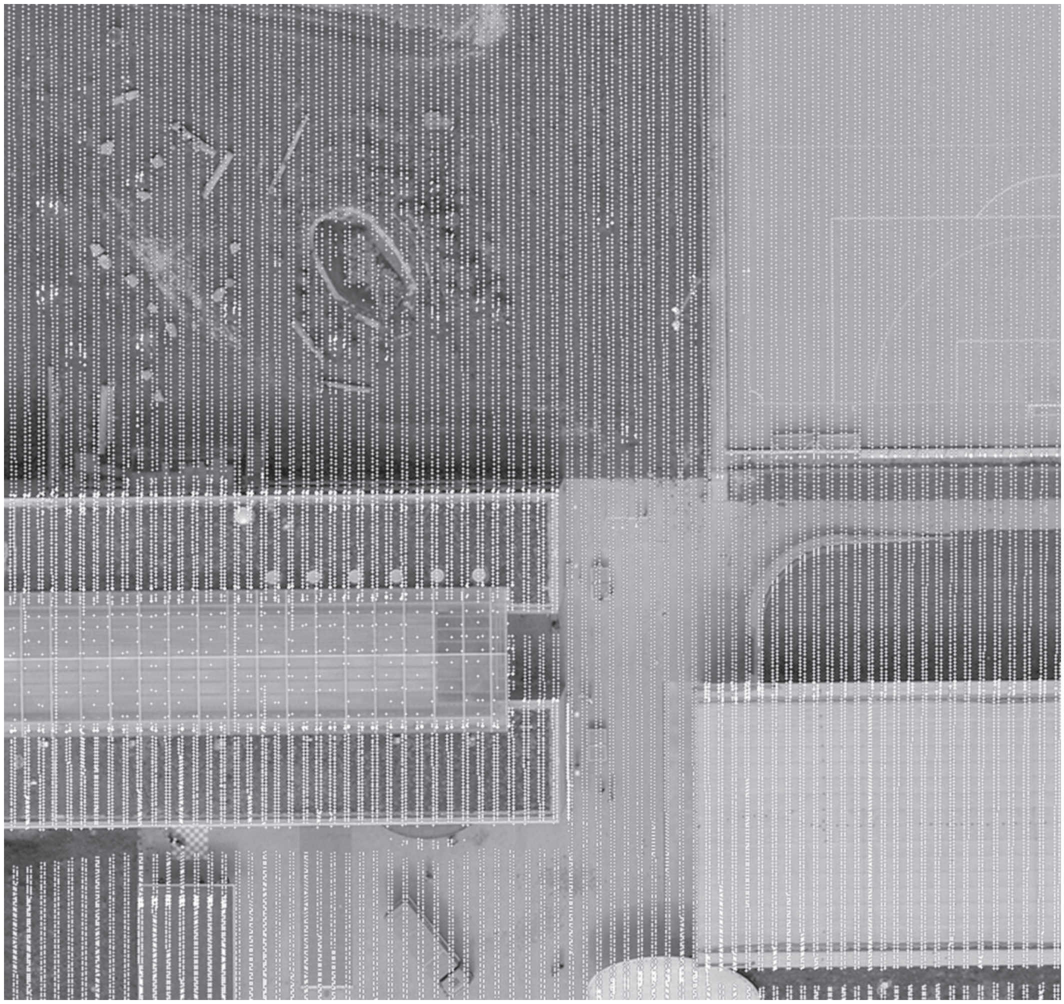

Figure 5. Section of UltraCam photograph at GSD 8 cm. Superimposed Leica Geosystems ALS50 lidar points at 70 cm spacing in the forward direction and 45 cm across the flight (Courtesy of DGPF).

related to the GPS/IMU accuracy and the horizontal uncertainties of lidar. We have no verification of that accuracy in the given experiment. Generally one can find literature assigning the differential GPS/IMU vertical position accuracy a value in the range of ±20 cm, with best cases at perhaps ±3 cm.

Second is the accuracy along discontinuities. This is very much defined by the point density; the dense photogrammetric matches were achieved at a 2-pixel interval and are thus at 25 points/m^2. The lidar resulted in 6 points/ m^2. It is visually obvious from Figure 6 how the roof line's definition is superior in the photogrammetric data set.

Third is the vertical data noise. Ideally, this should be in the range of the AT's uncertainty when surface points are being computed from all images and when surface texture is good. One would expect vertical noise in the range of the AT accuracy at ±3 cm. The flat soccer field in Figure 5 offers an experimental measure of noise, separate from the AT-derived value. The photogrammetric data show an uncertainty of slightly better than one pixel, at ±7 cm, which is more than expected. We assume that this error is caused by a failure to take advantage of all 10 images available to the matching process. Add-on research is needed to develop a full understanding of the effect of various approaches to multi-view matching and multi-view geometric processing on the creation of multi-image elevation measurements. The same soccer-field approach applied to the lidar data produces a deviation of ±2 cm from a regression plane. This error measurement ignores any horizontal error and any error of the GPS/IMU component. Those would need to be added to be comparable to a result from a triangulated image block. However, the photogrammetric accuracies scale with pixel size. Using a smaller pixel will improve the elevation noise. Therefore either a transition to a camera with yet more geometric resolution such as the UltraCamXp (note that the values quoted here are from the UltraCamX) or a lower flying height will achieve this improvement.

In summary the experimental evidence suggests that data from a fully digital photogrammetric workflow offer more detail at a comparable geometric accuracy than one can get from an aerial lidar-system.

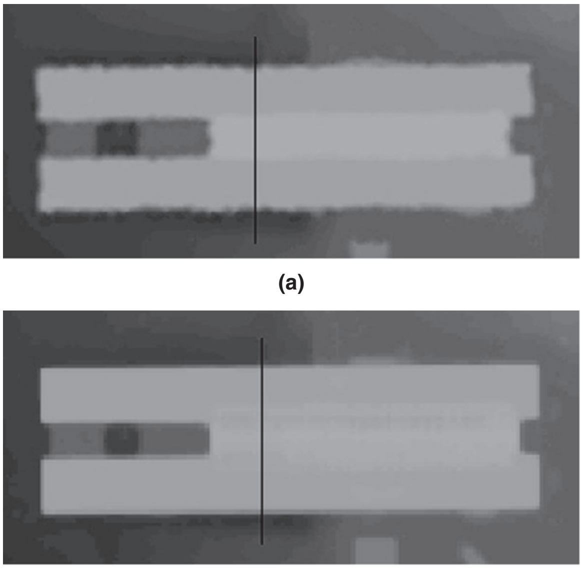

(a)

(b)

Figure 6. (a) ALS lidar at 45 cm spacing, and (b) photogrammetric image-based 3D at 16 cm spacing.

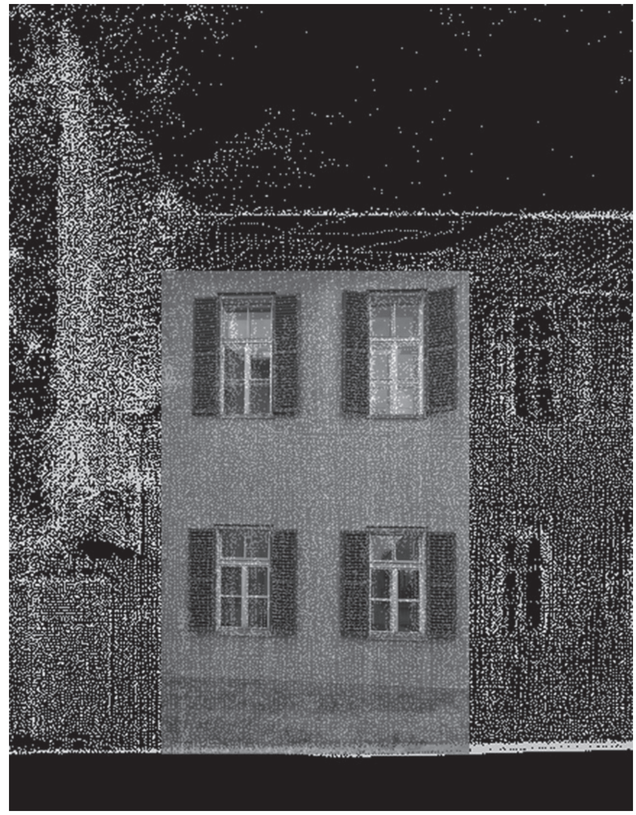

Figure 8. 60 laser points/m^2 and 6,000 image pixels/m^2.

Streetside Photogrammetric Dense Matching and Kinematic Lidar

We have repeated the aerial data analysis with terrestrial data collected for this research. Figure 7 is the result of a moving, thus kinematic, lidar survey of some streets, commercially contracted with the British provider StreetMapper (Kremer and Hunter, 2007; StreetMapper, 2009). Figure 8 superimposes over a street-side photo the lidar points of the same area. The photography was collected from a car with high overlap and with a pixel size that in this instance is 1.3 cm or 6,000 points/m^2. The lidar produces 1 percent of the data from a single image, namely 60 points/m^2.

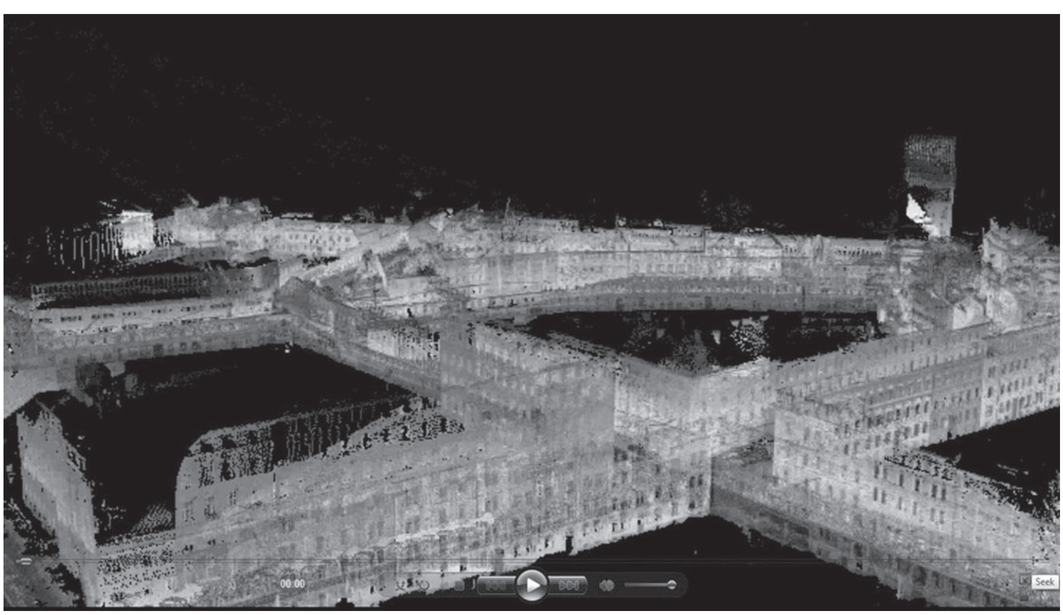

Figure 7. Laser scan of city streets obtained with the Street-Mapper (UK).

Figure 9. Scene for an automated point cloud from street side imagery with a pixel size of 1.3 cm

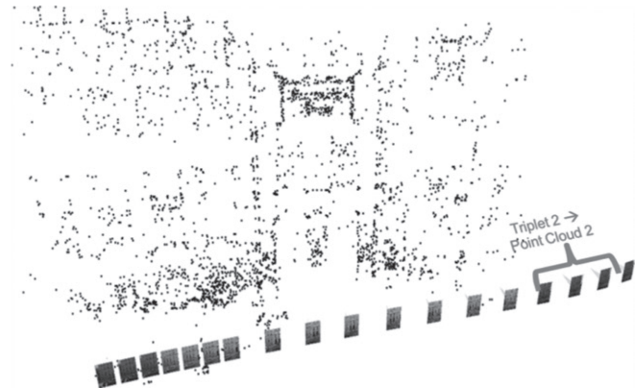

Figure 10. Automated AT connects 18 images with very high overlap in the selected scene (Figure 9).

Figure 11. Point cloud from image triplet of the scene in Figure 8, processed on PC with one GPU in 2 seconds.

To assess the image-based, photogrammetric 3D point generation workflow, we selected a façade (Figure 9). We led the imagery through a triangulation without any prior assumptions about the exterior orientation of the cameras (Irschara *et al.*, 2007), followed by a dense match on a GPU-supported PC using overlapping triplets (Zach, 2007). Figure 10 illustrates the result of the triangulation with its sparse point cloud and the arrangement of triplets for the 18 images overlapping a certain façade to produce the dense matches. Figure 11 is one point cloud patch from one of the 16 triplets, and Figure 12 is the resulting complete point cloud obtained by fusing the 16 patches using a robust fusion method (Zach *et al.*, 2007). The approach selected here did not take advantage of the stronger intersection geometry between non-neighboring images. We will investigate those benefits in a separate effort.

We have four passes of the lidar scanner over the façade shown in Figure 9. This supports an analysis of the differences in depth at ±1.7 cm among the four passes. Looking at a flat surface patch, we can determine from Table 2 that each lidar point cloud has noise at ±2 cm; this is consistent with the manufacturer's stated specification. This excludes consideration of the limitations of GPS/IMU pose measurements that may get compromised in narrow street canyons. This needs to be related to the photogrammetry result. The error of the mean is represented by an error of the triangulation, typically within a pixel or ±1.3 cm. The noise of the photogrammetric points is assessed in the same way as the lidar's and is found to be at ±0.9 cm. The experiment supports the conclusion that the photogrammetric data are superior to lidar data.

Low Cost Storage, High Level Automation, Graphics Processing Units

A superior photogrammetric process is feasible, but has yet to achieve acceptance as the technology of choice for the production of point clouds. While image-relevant innovations have been achieved in the camera domain, corresponding improvements of the image analysis solutions stalled. Academic work focused on processing lidar point clouds.

Figure 12. Fusion result obtained from 16 separately computed patches of point clouds, each from its triplet.

Table 2. Discrepancies in Four Street-side Lidar Runs in cm from the Area in Figure 9. Delta-Values: RMS Deviations from Regression Plane. Deviations of the Mean: Differences between Four Passes

LASER POINTS	Delta in [cm]	Deviations of the Mean [cm]
Krones-School, Pass A	2.09	(0.66)
Krones-School, Pass B	1.28	(2.39)
Krones-School, Pass C	1.60	1.20
Krones-School, Pass D	1.22	1.84
DELTA OF ALL PASSES	1.59	
R.M.S.E. OF THE MEANS		1.66

Leading industrial vendors saw their economic advantage in sales of lidar-systems, not in the development of software to improve image-based solutions beyond lidar's capabilities. Competitive end-to-end automated 3D vision workflows therefore are still a largely untapped entrepreneurial opportunity.

To bring the photogrammetric approach to fruition, three concerns need to be dealt with. First is the concern about high image overlap to result in a data overload. To counter, one needs to point to the cost of storage that over the recent 3 decennia has eroded at a rate of 12 million; this exceeds the improvement predicted by the rule of Moore (1965). Today a Terabyte disk is available for 125 USD (100 EUR). Clearly, storage therefore can no longer be considered a bottleneck of digital end-to-end workflows.

Second is the concern that (a) photogrammetry needs an AT and lidars do not, and (b) that an AT consumes manual labor and therefore per-image variable costs. To counter, one needs to emphasize that an AT produces sub-pixel accuracy and GPS/IMU-data do not. One will additionally need to recognize that AT manual labor is a function of the level of automation one achieves. The recent introduction of a fully automated AT (in the form of the UltraMap-AT software) demonstrates that this concern no longer applies (Reitinger and Gruber, 2009; Hui, 2009). Finally, the AT with images resembles post-processing of lidar-strips into a seamless data set with a difference: lidar strip adjustment has yet to be demonstrated in a fully automated work flow.

Third is the concern that dense matching of images is a slow process at a rate of perhaps one hour per large format digital image (at $17.5^K \times 11.5^K$ pixels). Dense matching of the 3,000 images for a 150 km^2 city would be processed in 3,000 hours or 125 days. To cope, some photogrammetric practitioners have embarked on so-called blade computers with many CPUs, even hundreds, per system (see for example the Verari blade system at **www.verari.com**). Space and energy consumption, as well as the cost of maintaining such systems, are seen as obstacles to success.

However, there exists an innovation that diminishes these constraints gracefully in the form of the GPU, with the CUDA-software to program such graphics processors for general purpose applications. The illustrations in Figures 11 and 12 present point clouds per image triplet. The processing takes one to three seconds on a PC augmented by a single GPU. We have great expectations that with up to four current GPUs per PC, one can achieve an acceleration of up to 400 over an unaided PC. A simple PC with 4 GPUs hosting some dense matching software should eliminate the concern over excessive computing times since with such a system the city project would be matched not in 125 days, but in a single eight-hour shift.

Advantages of Fully Automated 3D Vision Aerial Mapping

Table 3 summarizes the 16 advantages of the photogrammetric approach over the lidar approach. An important factor is the well-documented need for a lidar to be augmented by imagery to have the much-appreciated photographic texture. This results in the complication of a dual workflow, i.e., the first one with a lidar and a second one with a lower cost digital camera operated without any stereo considerations. This "active imaging" requires a match between the lidar and image data, a non-trivial effort (Habib *et al.*, 2005). By contrast, the strictly image based approach needs only one single workflow and creates point clouds using image correspondences, and operates with multiple image textures. An often-heard observation is that lidar has its own application and digital aerial photography has another; oftentimes these technologies do supplement one another. However, this observation typically ignores the issue of economy and suggests that one should maintain both a digital aerial camera sensor and processing workflow as well as a lidar sensor with attached digital camera and associated workflow. How can this be justified when one single system and workflow would suffice?

When a point cloud is not a data product in its own right, but a source for mapping topographic objects, one is faced with the need to extract such objects. Not using image texture makes this a challenging endeavor, as one can easily appreciate, for example when looking for windows (Ali, 2009).

Two unique advantages or unique selling propositions (USP) of lidar were previously mentioned. First is the ability to look between leaves of trees onto the ground and thus to

Table 3. Sixteen Advantages of the Photogrammetric 3D Workflow over the Directly Measured Laser Point Clouds

Accuracy and Errors	
1.	Large area rigid camera image block geometry via AT at a sub-pixel accuracy
2.	Error checking using redundant observations as a system-inherent verification
3.	Internal accuracy measures from redundancy
4.	Geometric accuracy by AT superior to a reliance on GPS/IMU to fuse patches into seamless coverage
5.	Greater point density → for better defined discontinuities
Economy	
6.	Superior data collection efficiency with faster vehicles, larger swaths
7.	Single workflow within aerial application, all image-based
8.	Single workflow across widely varying applications (aerial, street-side & indoor)
9.	No occlusions using no-cost along-track high image overlaps
Data Types	
10.	2D-image information augmenting 3D data points
11.	Multi-spectral image classification
12.	Urban façade textures available at no cost from the air at image edges
13.	Images document details → example street signs can be read automatically
Miscellaneous	
14.	*Perspective exists towards Real time 3DVision* via "*supercomputer in match box"*
15.	Full automation needs image redundancy → lidar adds little to automation
16.	Scene interpretation is becoming important and needs imagery → lidar adds little

provide multiple reflections of the laser so that a bald earth terrain model (DTM) as well as a surface model (DSM) can be produced with ease. Second is the capability to see suspended wires. Research to assess the uniqueness and importance of these advantages is needed. One will find that with an intelligent analysis of image content, one will be able to define a bald earth and its vertical objects from overlapping images. This may erode some of the lidar USP.

Street Imagery

The appetite for detail justifies an augmentation of aerial mapping by street-level and indoor mapping. Commercial solutions have been developed in significant numbers for lidars to map streets (Figure 7), and indoor spaces such as tunnels (Kremer and Hunter, 2007; Streetmapper, 2009; Leica Geosystems, 2008b, Zoller+Fröhlich, 2007). Camera solutions also exist for these applications (Cyclomedia, 2008; Facet Technology, 2008). The workflow and technology issues from airborne work transfer into these new street level applications. But while a comparison between the use of street-side (and indoor) lidars and of blocks of overlapping street-level and indoor digital images is of great interest, it has not been widely studied. One effort was by Strecha *et al.* (2008) using lidar data (Zoller+Fröhlich IMAGER 5003 laser scanner) as ground truth to assess computer vision results. The authors show that current fully-automated Structure-from-Motion pipelines like that by Martinec *et al.* (2007) achieve a camera calibration accuracy close to the 3σ-value of the lidar ground truth. Our contribution in this paper sharpens that conclusion by a quantitative system accuracy evaluation resulting in better image-based results than lidar.

Qualitative Considerations

Besides the geometric accuracy and the concerns for the economy of data acquisition, there exist various qualitative issues to consider in a comparison:

- Maintaining single workflows in lieu of separate workflows will be commercially attractive, particularly if the uniform workflows are applicable across various mapping scenarios, be they a project with aerial imagery, or street-side imagery, or perhaps even inside a building from indoor imagery.
- Images document the details of street sides and indoor scenes. The examples with street signs and alpha numeric information on facades are important.
- The interpretability of objects from imagery as a computer vision task relies on imagery. Images are therefore unavoidable, and redundancy is also unavoidable. The lidar may not add much value to a block of street side or indoor images when an automated workflow for 3D vision is in use to build models of all objects for subsequent selective visualiztion.

Conclusions

Grün (2009) has argued that statements about the demise of photogrammetry are premature. In doing so he confirmed an unease in photogrammetry about the field. With the advent of 3D point clouds as a mapping data product for the new world of 3D visualizations, photogrammetry was not able to be the preferred technology; lidar took that place. We have developed experimental evidence that point clouds created by softcopy photogrammetry compare favorably with those from lidar. In the process we support Grün's vision that photogrammetry better not be discounted as the better technology for point cloud measurements.

We are investigating the geometric accuracy and point densities from airborne and street-side lidar scanners versus highly overlapping imagery and fully automated image-based photogrammetry. While it was fully understandable that lidar scanning was advantageous over traditional film-based 3D photogrammetry, that advantage goes away as photogrammetry morphs into 3D vision based on a fully digital, automated workflow on GPU-augmented computers. We can show that in aerial situations, the accuracy of 3D-vision points is often better than ±1 pixel, whereas the lidar accuracies are defined by the direct georeferencing from GPS/IMU measurements. Aerial point densities favor the image-derived data over the direct lidar observations. In the application to street-scenes, the data densities differ more strongly. The image-based data may be 100 times richer than the lidar points while the geometric accuracies are shown to be in the same range with noise values at ±1 to ±2 cm.

Apart from the geometric parameters of these technologies, there are numerous economic considerations as well as considerations concerning the richness of the information content. These all favor the image-based approach. With an aerial camera, a flying mission may be completed in 10 percent of the time a lidar takes. In street-side applications, the ability to identify signs, to interpret the scenes, to track their changes and to be much less dependent on directly measuring the sensor pose in narrow street canyons may be an invaluable advantage over the simple collection of point clouds with a direct pose measurement.

Acknowledgments

Support was provided by Microsoft's A. Klaus (Dense Match), and B. Reitinger and B. Schachinger (Aero-Triangulation). At Graz University of Technology, support was by project grants "*wikivienna*" (A. Irschara) and "*VM-GPU 813396*" (T. Pock). Project GeoVis of VRVis GmbH (Vienna) funded P. Meixner.

References

Ackermann, F., 1993. Application of GPS for aerial triangulation, *Photogrammetric Engineering & Remote Sensing*, 29(1):691–700.

Agüera y Arcas, B., 2007. URL: *http://www.ted.com/talks/blaise_aguera_y_arcas_demos_photosynth.html*, (last date accessed: 12 July 2010)

Ali, H., R. Sablatnig, and G. Paar, 2009. Window detection from terrestrial laser scanner data, *Proceedings of VISAPP-2009- 4th International Conference on Computer Vision Theory and Applications*, Lisbon, pp. 393–397.

ASPRS, 2009. *Photogrammetric Engineering & Remote Sensing*, American Society for Photogrammetry and Remote Sensing.

Balce, A., 1986. Determination of optimum sampling interval in grid digital elevation models data acquisition, *Proceedings ISPRS Commission III Symposium*, Finland, *International Archives of Photogrammetry and Remote Sensing*, 26(3.1):40–55

Bauer, J., 2009. *Feature-Based Reconstruction of 3D Primitives from Multiple Views*, Doctoral Thesis, Graz University of Technology, 187 p.

Baltsavias, M., 1999. A comparison between photogrammetry and laser scanning, *ISPRS Journal of Photogrammetry and Remote Sensing*, Vol. 54, pp 83–94

Beasy, C., 2007. Lidar and Photogrammetry, How Do I Choose?, Eagle Mapping, URL: *http://www.eaglemapping.com/publications/Lidar%20-%20Photo%20Article.pdf* (last date accessed: 12 July 2010).

Bitelli, G., M. Dubbini, and A. Zanutta, 2004. Terrestrial laser scanning and digital photogrammetry techniques to monitor landslide bodies, *International Archives of Photogrammetry, Remote Sensing and Spatial Information Sciences*, XXXV, Part B, pp. 246–251.

Champion, N., F. Rottensteiner, L. Matikainen, X. Liang, J. Hyyppä, and B. P. Olson, 2009. A test of automatic building change detection approaches, *Proceedings of CMRT09* (U. Stilla, F. Rottensteiner, and N. Paparoditis, editors) 03–04 September, *International Archives of the ISPRS*, Vol. XXXVIII, Part 3/WG4, pp. 145–150 (available from GITC, Lemmer, The Netherlands).

Choma, A, C. Ratcliff, and R. Frisina, 2005. Evaluation of remote sensing technologies for high-resolution terrain mapping. *Proceedings of SSC 2005*, Spatial Sciences Institute, Melbourne, Australia, ISBN 0-9581366-2-9, pp 751–760.

Cramer, M., and N. Haala, 2009. DGPF project: Evaluation of digital photogrammetric aerial based imaging systems - Overview and results from the pilot centre, *Proceedings of the ISPRS Workshop on High-Resolution Earth Imaging for Geospatial Information*, ISPRS Archives, Vol. XXXVIII-1-4-7/W5, ISSN 1682–1777, Leibniz-University Hannover, Germany, 02–05 June, URL: *http://www.ipi.uni-hannover.de/322.html* (last date accessed: 12 July 2010).

Cyclomedia, 2008. URL: *http://www.cyclomedia.nl/* (last date accessed: 12 July 2010).

Facet Technology, 2008. URL: *http://www.facet-tech.com/* (last date accessed: 12 July 2010).

DGPF, 2009) *Photogrammetrie, Fernerkundung, Geoinformation*, Journal of the German Society for Photogrammetry, Remote Sensing and Geoinformation DGPF (H. Mayer, editor), Schweizerbart'sche Verlagsbuchhandlung, Stuttgart.

Gruber, M., and R. Ladstätter, 2006. Geometric issues of the digital large format aerial camera UltraCamD, *Proceedings of the International Calibration and Orientation Workshop EuroCOW*, 25–27 January, Castelldefels, Spain, unpaginated CD-ROM.

Gruber, M., and B. Reitinger, 2008. UltraCamX and a new way of photogrammetric processing, *Proceedings of the ASPRS 2008 Annual Convention*, Portland., Oregon, unpaginated CD-ROM.

Grün, A., 2009. Photogrammetry - Revival of a discipline, *GIS Development*, Vol. 1, pp. 30–31.

Grün, A., 2007. Laser scanner blackbox or braintwister?, *GEOInformatics*, 10(7):49.

Haala, N., K. Wolff, 2009. Digitale photogrammetrische Luftbildkamerasysteme - Evaluation der automatischen Generierung von Höhenmodellen, *Proceedings of the Annual Meeting of the DGPF (German Society for Photogrammetry and Remote Sensing)*, Publication of the DGPF, Volume 18, ISSN 0942–2870, Eckhardt Seyfert, Publisher, pp 23–32.

Habib, A., M. Ghanma, and E.-M. Kim, 2005. Lidar data for photogrammetric georeferencing, From Pharaos to Geoinformatics, *Proceedings of the FIG Work Week 2005*, Cairo, Egypt, 15 p., URL: *http://www.fig.net/pub/cairo/papers/ts_38/ts38_04_habib_etal.pdf* (last date accessed: 12 July 2010).

Hartley, R, and A. Zissermann,2004. *Multiple View Geometry for Computer Vision*, Cambridge University Press, Second edition, 672 p.

Hirschmugl, M., 2008. *Derivation of Forest Parameters from UltracamD Data*, Doctoral Thesis, Graz University of Technology, 238 p.

Hui, J., 2009. *Optimization and Evaluation of the Microsoft Automatic Aerial Triangulation Software Package*, Diploma Thesis, University Stuttgart, Institute for Photogrammetry, *http://www.ifp.uni-stuttgart.de/lehre/diplomarbeiten/ju/ju.html* (last date accessed: 12 July 2010).

ILMF, 2009. International Laser Mapping Forum 2009, New Orleans, URL: *http://www.lidarmap.org/* (last date accessed: 12 July 2010).

Irani, M., and S. Peleg, 1991. Super resolution from image sequences, *Proceedings of the International Conference on Pattern Recognition ICPR*, Vol 2, pp 15–120

Irschara, A., C. Zach, and H. Bischof, 2007. Towards Wiki-based dense city modeling, *Proceedings of the Eleventh IEEE International Conference on Computer Vision, Workshop on Virtual Representations and Modeling of Large-scale Environments (VRML)*, pp. 1–8, URL: *http://ieeexplore.ieee.org/xpl/freeabs_all.jsp?arnumber=4409216* (last date accessed: 12 July 2010).

ISPRS, 2008. The International Archives of the Photogrammetry, Remote Sensing and Spatial Information Sciences, *Proceedings of the 31st ISPRS Congress Beijing 2008*, Volume XXXVII, ISSN 1682–1750.

Kaartinen, H., J. Hyyppä, E. Gülch, G. Vosselman, H. Hyyppä, L. Matikainen, A.D. Hofmann, U. Mäder, Å. Persson, U. Söderman, M. Elmqvist, A. Ruiz, M. Dragoja, D. Flamanc, G. Maillet, T. Kersten, J. Carl, R. Hau, E. Wild, L. Frederiksen, J. Holmgaard, and K. Vester, 2005. Accuracy of 3D city models: EurosSDR comparison. *Proceedings of ISPRS WG III/3, III/4, V/3 Workshop "Laser Scanning 2005"*, Enschede, Netherlands, pp 227–232

Klaus, A., 2007. *Object Reconstruction from Image Sequences*, Doctoral Thesis, Graz University of Technology, 178 p.

Kraus, K., 2004. *Photogrammetrie*, Vol. I., Seventh Edition (516 pages), Vol. II, Third Edition (488 pages), Walter de Gruyter Verlag, Berlin-New York.

Kremer, J., and G. Hunter, 2007. Performance of the Street-Mapper Mobile LIDAR mapping system, Real world projects, *Proceedings of the Photogrammetric Week 2008*, Wichmann Verlag, pp. 215–225.

Ladstädter R., and M. Gruber, 2008. Geometric aspects concerning the photogrammetric work flow of the digital aerial camera UltraCamX, *Proceedings of the 21st ISPRS Congress Beijing 2008, International Archives of Photogrammetry, Remote*

Sensing and Spatial Information Sciences, Vol. XXXVII, ISSN 1682–1750, pp.521–525.

Leica Geosystems, 2008a. Leica Airborne Laser Scanner ALS60, URL: *http://www.leica-geosystems.com/us/en/lgs_57629.htm* (last date accessed: 12 July 2010).

Leica Geosystems, 2008b. Leica Scan Station 2, URL: *http://www.leica-geosystems.com/hds/en/lgs_62189.htm* (last date accessed: 12 July 2010).

McGlone, C., E.M. Mikhail, J. Bethel, and R. Mullen, 2004. *Manual of Photogrammetry*, Fifth Edition, American Society for Photogrammetry and Remote Sensing, 1151 pages.

Microsoft Livelabs, 2009. Seadragon, URL: *http://livelabs.com/seadragon/* (last date accessed: 12 July 2010).

Martinec, D., and T. Pajdla, 2007. Robust rotation and translation estimation in multi-view reconstruction, *Proceedings of the IEEE Conference on Computer Vision and Pattern Recognition,* CVPR, 8 p.

Moore, G.E., 1965. Cramming more components onto integrated circuits, *Electronics*, Volume 38, Number 8, URL: *http://download.intel.com/museum/Moores_Law/Articles-Press_Releases/Gordon_Moore_1965_Article.pdf* (last date accessed: 12 July 2010).

Optech, Inc., 2009. Optech Announces New ALTM Technology Platform - The Pegasus HD400 Active Imaging System, URL: *http://www.optech.ca/091110_new_altm_platform.html* (last date accessed: 12 July 2010).

Perko, R.,2004. *Computer Vision For Large Format Digital Aerial Cameras*, PhD Thesis, Graz University of Technology, 174 p.

Perko, R., A. Klaus, and M. Gruber, 2004. Quality comparison of digital and film-based images for photogrammetric purposes, *International Archives of Photogrammetry, Remote Sensing and Spatial Information Sciences, ISPRS Commission III: Theory and Algorithms*, Volume XXXV(B3):1136–1140.

Petrie, G., 2009. Current Developments in Laser Scanning Technologies, *Proceedings of the IX International Scientific & Technical Conference: From Imagery to Map: Digital Photogrammetric Technologies,* Attica, Greece, 05–08 October, URL: *http://web2.ges.gla.ac.uk/~gpetrie/* (last date accessed: 12 July 2010).

Reitinger, B., M. Hoefler, A. Lengauer, R. Tomasi, M. Lamperter, and M. Gruber,2008. Dragon fly - Interactive visualization of huge aerial image datasets, *Proceedings of the 31st ISPRS Congress Beijing 2008, International Archives of Photogrammetry, Remote Sensing and Spatial Information Sciences*, pp. 491–494.

Schickler, W., and A.Thorpe, 2001. *Surface estimation based on LIDAR*, *Proceedings of the 2001- ASPRS Annual Convention*, St. Louis, Missouri, unpaginated CD-ROM.

Scholz, S., and M. Gruber, 2008. Radiometric Quality of UltraCam Images. *Proceedings of the 21st ISPRS Congress Beijing 2008, International Archives of Photogrammetry, Remote Sensing and Spatial Information Sciences*, ISSN 1682–1750, pp.539–543.

Scholz, S., and M. Gruber, 2009. Radiometric and geometric quality aspects of the large format aerial camera UltraCam-Xp, *Proceedings of the ISPRS Workshop on High-Resolution Earth Imaging for Geospatial Informatio*n, XXXVIII-1-4-7/W5, ISSN 1682–1777, Leibniz-University Hannover, Germany, 02–05 June 2, URL: *http://www.ipi.uni-hannover.de/322.html* (last date accessed: 12 July 2010).

Shan, J., and C. Toth (editors), 2009. *Topographic Laser Ranging and Scanning*, CRC Press, Taylor and Francis Group, 590 p.

Strecha, C., W. von Hansen, L. Van Gool, P. Fua, and U. Thoennessen, 2008. On benchmarking camera calibration and multi-view stereo for high resolution imagery, *Proceedings of the IEEE Conference on Computer Vision and Pattern Recognition CVPR.*, pp 1–8, URL: *http://cvlab.epfl.ch/~strecha/publications/strecha_cvpr_2008.pdf* (last date accessed: 12 July 2010).

StreetMapper, 2009. *URL: http://www.streetmapper.net/* last date accessed: 12 July 2010).

Veneziano, D., 2002. Accuracy evaluation of LIDAR-derived terrain data for highway location, URL: *http://www.veejam.com/Guyana/Veneziano.pdf* (last date accessed: 12 July 2010).

Veneziano, D., S. Hallmark, and R. Souleyrette, 2002. *Comparison of Lidar and Conventional Mapping Methods for Highway Corridor Studies*, Final Report, Center for Transportation Research and Education, Iowa State University, URL: *http://www.intrans.iastate.edu/reports/lidar_comparison.pdf* (last date accessed: 12 July 2010).

Wang, T., Q. Abdullah, D. Chavez, R. Kandukuri, N. Csanyi-May, and D. Simerlink, 2009. The quality of one-foot contour modeling using lidar data versus photogrammetrically-derived solutions, *Proceedings International Lidar Mapping Forum,* January, New Orleans, Louisiana, unpaginated CD-ROM, 9 p.

Wiechert, A., and M. Gruber, 2009. Aerial perspective: Photogrammetry versus lidar, *Professional Surveyor Magazine*, August, *http://www.profsurv.com/magazine/article.aspx?i=70305* (last date accessed: 12 July 2010).

Zach, C., 2007. *High-Performance Modeling From Multiple Views Using Graphics Hardware*, Ph.D. Thesis, Graz University of Technology, 184 p.

Zach, C., T. Pock, and H. Bischof, 2007. A globally optimal algorithm for robust TV-L^1 range image integration, *Proceedings of the Eleventh IEEE International Conference on Computer Vision*, pp. 1–8, URL: *http://ieeexplore.ieee.org/xpl/freeabs_all.jsp?arnumber=4408983* (last date accessed: 12 July 2010).

Zebedin, L., A. Klaus, B. Gruber-Geymayer, and K. Karner, 2006. Towards 3D map generation from digital aerial images, *ISPRS Journal of Photogrammetry and Remote Sensing*, 60(6):413–427.

Zebedin, L, T. Pock, A. Klaus, K. Karner, and H. Bischof, 2009. *A TV-L1 Method for Robust Fusion of 2.5D Range Images*, Technical Report, Institute for Computer Graphics and Vision, Graz University of Technology, URL: *www.gpu4vision.org* (last date accessed: 12 July 2010).

Zoller + Fröhlich, 2007. URL: *www.zf-laser.com* (last date accessed: 12 July 2010).

(Received 23 July 2009; accepted 16 December 2009; final version: 22 January 2010)